Joule–Thomson Inversion Curves and Third Virial Coefficients for Pure Fluids from Molecular-Based Models

ARTICLE *in* INDUSTRIAL & ENGINEERING CHEMISTRY RESEARCH · SEPTEMBER 2008

Impact Factor: 2.59 · DOI: 10.1021/ie800651q

3 AUTHORS, INCLUDING:

Claudio Olivera-Fuentes
Simon Bolívar University
60 PUBLICATIONS **255** CITATIONS
SEE PROFILE

Coray M Colina
University of Florida
85 PUBLICATIONS **697** CITATIONS
SEE PROFILE

Article

Joule#Thomson Inversion Curves and Third Virial Coefficients for Pure Fluids from Molecular-Based Models

F. Castro-Marcano, C. G. Olivera-Fuentes, and C. M. Colina

Ind. Eng. Chem. Res., **2008**, 47 (22), 8894-8905 • Publication Date (Web): 27 September 2008

Joule−Thomson Inversion Curves and Third Virial Coefficients for Pure Fluids from Molecular-Based Models

F. Castro-Marcano,[†,‡] C. G. Olivera-Fuentes,[‡] and C. M. Colina*[,†]

Department of Materials Science and Engineering, The Pennsylvania State University, University Park, Pennsylvania 16802, and TADIP Group, Thermodynamics and Transport Phenomena Department, Simón Bolívar University, Caracas 1080, Venezuela

In this work, we present the application of the BACKONE, PC-SAFT, SAFT-VR, and soft-SAFT models to examine the impact of the accuracy of representation of third virial coefficients on the behavior of the correspondingly predicted Joule−Thomson inversion curve (JTIC). Calculations were performed for nonassociating fluids such as ethane and pentane, associating fluids such as alcohols, and quadrupolar fluids such as nitrogen and carbon dioxide. By taking advantage of the molecular nature of the models investigated, we were able to evaluate the separate contributions to the Helmholtz free energy. Nonassociating and quadrupolar fluids are mostly governed by the dispersion contribution, whereas, as expected, the association term plays a predominant role for associating compounds. We validated our previous findings that deviations from the correct shape of the JTIC at high temperatures directly reflect the inadequacies in the predicted third virial coefficients. Consequently, much attention should be dedicated to the reliable description of virial coefficients in building and testing any newly developed equation of state.

1. Introduction

Knowledge of the inversion curve, defined as the locus of points where the Joule−Thomson coefficient becomes zero, plays a key role in the design and operation of throttling processes. For instance, in refrigeration and liquefaction processes, the fluid temperature can either increase or decrease depending on the pressure and temperature conditions for an isenthalpic fluid expansion. The heating and cooling regions can be identified by inspection of the respective Joule−Thomson inversion curve (JTIC). Similarly, in petroleum and gas reservoirs at extremely high pressures and temperatures, knowledge of the JTIC permits a qualitative explanation of unexpected changes in temperature of the reservoir fluid rising through the wellbore.[1] According to a recently proposed theoretical model, inversion phenomena also play an important role in the flow of reservoir fluids through porous media.[2]

Despite their relevance in these and other industrial applications, experimental determination of a JTIC is extremely difficult because of the severe experimental conditions involved (often up to five times critical temperature and 12 times critical pressure). Hence, experimental inversion curve data are rather scarce and often unreliable. According to the available experimental information, in a temperature−pressure diagram, the JTIC is expected to extend from a minimum temperature corresponding to a saturated state to a maximum temperature where both the density and pressure approach zero. The shape of the JTIC is parabolic, with a maximum inversion pressure at an intermediate temperature. An alternative method to circumvent the difficulties associated with the experimental determination of the inversion points has been the use of molecular simulations. Monte Carlo simulation methods in the isothermal−isobaric ensemble have satisfactorily predicted the inversion curves for Lennard-Jones (LJ) fluids,[3,4] carbon dioxide,[5−7] light *n*-alkanes[8−10] and their mixtures,[8] and condensate gases,[11] and simulations in the isenthalpic−isobaric ensemble have predicted those for difluoromethane[12] and hydrogen sulfide.[13] The use of a molecular-based equation of state (EoS) is also an attractive option because such equations can provide rapid and reliable JTIC calculations through thermodynamic relations. In fact, the estimation of the JTIC represents one of the strongest tests for any EoS, as it demands an accurate description of both temperature and volume derivatives of pressure. The most commonly used formulation of the inversion condition for predicting JTICs from an EoS is given by

$$T\left(\frac{\partial P}{\partial T}\right)_v + v\left(\frac{\partial P}{\partial v}\right)_T = 0 \tag{1}$$

where T, P, and v are the temperature, pressure, and molar volume of the fluid, respectively. A large number of studies have reported the use of EoSs for the estimation of JTICs since Miller's work in 1970.[14] Nichita and Leibovici[15] recently found that cubic EoSs commonly used for engineering applications are able to predict qualitatively the entire JTIC, which is particularly remarkable considering that most cubic equations are normally developed by performing local fits of phase equilibria. Previously, we applied[16] a molecular-based EoS, the soft-SAFT approach, to predict JTICs for carbon dioxide (CO_2) and *n*-alkanes. The influence of molecular parameters on predictions of the JTIC was studied by using three different sets of parameters available for *n*-alkanes with such an EoS. In that work, we showed that the accuracy of JTIC predictions in the high-temperature region depends strongly on the set of molecular parameters used.

Additionally, we have shown[17] that, for low pressures and high temperatures, the inversion density can be expressed in terms of the second and third virial coefficients. Accordingly, the accurate description of the inversion behavior at higher temperatures depends on the capacity of the EoS to provide correct virial coefficients. We demonstrated in particular that the deformation of the JTIC computed from the multiparameter EoS for CO_2 developed by Pitzer and Sterner[18] takes place over the same range of temperatures where the respective third virial

* To whom correspondence should be addressed. E-mail: colina@matse.psu.edu.
† Pennsylvania State University.
‡ Simón Bolívar University.

10.1021/ie800651q CCC: $40.75
Published on Web 09/27/2008

coefficient goes to (incorrect) negative values. As a result, unphysical negative inversion density values are obtained when this EoS is used near the maximum inversion temperature. On the basis of those results, an analysis of third virial coefficients was suggested as a routine test for any EoS, especially those that are newly developed. In a similar context, Lemmon and Jacobsen[19] more recently found similar abnormal behaviors at high temperatures for JTICs computed from various empirical multiparameter EoSs for different fluids, including the prediction of unreasonable third virial coefficients. They found in general that the equations that behaved well for the third virial coefficient were able to predict the whole JTIC correctly. They also appeared to suggest that a verification of third virial coefficients should be a requirement in the development and testing of any new EoS.

The effects of inaccurate representation of third virial coefficients are not limited to the Joule−Thomson effect. Gas-phase thermodynamic properties in general will be affected. For instance, Chirico and Steel,[20] Steel et al.,[21] and Chirico et al.[22] demonstrated that third virial coefficients have a significant impact on calculations of enthalpies of vaporization and entropies derived from calorimetric and spectroscopic studies. Ichikura et al.[23] recently underlined the strong influence of the third virial coefficient in describing isochoric and isobaric heat capacities in the gaseous phase. Virial coefficients also provide a theoretical basis for obtaining simple and accurate estimates of the solubility of a solute in a supercritical fluid.[24−26] Moreover, the direct relation of third virial coefficients to intermolecular forces recently served to provide insight into the molecular interactions of protein solutions usually found in living cells.[27]

Experimental data on third virial coefficients have not been as plentiful and accurate as those on second virial coefficients because of instrumental and technical difficulties. In 2002, Dymond et al.[28] presented a new, critical, and comprehensive compilation of second and third virial coefficient data from different published sources up to the end of 1998. An alternative route to calculating virial coefficients is the use of theoretical models based on intermolecular potential functions. Both the LJ and the square-well potentials have been used to predict virial coefficients for nonpolar molecules,[29−32] whereas the two-center LJ (2CLJ) potential has been used for simple linear molecules, with improvements made by adding dipole (2CLJD model)[33−35] and quadrupole (2CLJQ model)[36−40] terms to the core LJ potential. Many empirical correlations have also been developed to determine virial coefficients. Corresponding-states correlations have been widely applied to third virial coefficients of nonpolar[41−43] and polar[44,45] substances. Formulations based on the second virial coefficient have also been employed for estimation of third virial coefficients for nonpolar and polar compounds.[46,47] Recently, the Clausius−Clapeyron equation was applied to calculate third virial coefficients at low reduced temperatures (from 0.8 to 1.0) for nonpolar fluids.[48]

Several studies have been performed using both cubic and empirical multiparameter EoSs to investigate the relation between the computed JTIC of a fluid and its respective third virial coefficients. However, to the best of our knowledge, similar systematic studies using molecular-based EoSs have not been reported in the literature. Consequently, the main goal of this work was to study the direct influence that properly predicted third virial coefficients from molecular-based models currently in use have on the correct shape of the upper-temperature region of the JTIC. To achieve this aim, we used the BACKONE[49] EoS and several versions of the SAFT[50] approach, based on their reference term: the soft-SAFT[51,52] EoS (LJ), the SAFT-VR[53,54] EoS (square-well), and the PC-SAFT[55] EoS (hard-chain). We used selected compounds as representative of each type of substances: ethane and pentane (nonassociating fluids), methanol (associating fluid), and nitrogen and carbon dioxide (quadrupolar fluids). The evaluation of the ability of molecular-based models to predict these properties might contribute to the extension of their application to different types of fluids and other thermodynamic properties.

2. Molecular-Based Models

Molecular-based EoSs account explicitly for the effects of molecular structure and interactions on the thermodynamic properties of fluids and fluid mixtures. Their rigorous basis in statistical mechanics allows a reliable representation of real fluids and mixtures over a wide range of temperatures and pressures. Hence, they have been applied to describe industrially important systems, such as electrolyte solutions, polymers and their mixtures, hydrocarbons, and surfactants. Detailed descriptions on modifications, extensions, and applications are given by Müller and Gubbins,[56] Wei and Sadus,[57] and Economou.[58] Brief descriptions of the BACKONE, soft-SAFT, SAFT-VR, and PC-SAFT models are given below. The reader is referred to the original publications for the details of each model.

The BACKONE[49] EoS is a modified version of the original BACK equation proposed by Chen and Kreglewski.[59] As in the original model, it uses a hard-convex body reference term with a temperature-dependent molecular volume. However, in this case, the dispersive contribution is expressed as a double power series in scaled density and temperature, derived by multivariable regression of data for methane, oxygen, and ethane. For pure fluids, the Helmholtz free energy, A, can be written as

$$\frac{A}{RT} = \frac{A^{\mathrm{ref}}}{RT} + \frac{A^{\mathrm{disp}}}{RT} + \frac{A^{\mathrm{QQ}}}{RT} \tag{2}$$

where R is the universal gas constant and T is the temperature. A^{ref} is the repulsion contribution (reference hard-body term), and A^{disp} is the dispersion contribution. The quadrupolar interactions are individually considered by the additional term A^{QQ}. In this model, molecules are treated as hard-convex bodies with characteristic density ρ_0, temperature T_0, and nonspherical shape (anisotropy) parameter α; these are the three molecular parameters used to model simple pure fluids. One extra adjustable parameter (Q^{*2}) must be included when dealing with quadrupolar fluids. Dipolar forces can also be considered through an additional term in eq 2. In this work, we do not study dipolar fluids, so this contribution is not necessary. It should also be noted that the effect of associating interactions is not explicitly taken into account in eq 2. Several authors[60−62] have shown that the BACKONE EoS is able to describe thermodynamic properties and phase equilibria of nonpolar, dipolar, and quadrupolar pure fluids and their mixtures. Recently, Wendland et al.[63] studied mixed natural gases using this model.

Within the SAFT[50] framework, the residual Helmholtz free energy, A^{res}, can be expressed as the addition of various contributions as

$$\frac{A^{\mathrm{res}}}{RT} = \frac{A^{\mathrm{ref}}}{RT} + \frac{A^{\mathrm{disp}}}{RT} + \frac{A^{\mathrm{chain}}}{RT} + \frac{A^{\mathrm{assoc}}}{RT} + \frac{A^{\mathrm{QQ}}}{RT} \tag{3}$$

where A^{ref} denotes the contribution due to the reference system (often modeled as hard-sphere, square-well, LJ, or hard-chain interactions), A^{disp} corresponds to the free energy due to the dispersion interactions between segments, A^{chain} accounts for the formation of chains, A^{assoc} is the contribution due to the

Table 1. Molecular Parameters for the Molecular-Based Models

EoS	m	σ (Å)	ϵ/k (K)	λ	ϵ^{HB}/k (K)	k^{HB} (Å^3)	Q (DÅ)	α	ρ_0 (mol/L)	T_0 (K)	Q^{*2}	ref
						Ethane						
BACKONE								1.2126	6.8000	305.33		49
soft-SAFT	1.3920	3.7560	202.50									103
SAFT-VR	1.2400	3.9080	264.20	1.418								53
PC-SAFT	1.6069	3.5206	191.42									55
						Pentane						
BACKONE								1.4011	3.1407	448.96	2.3962	63
soft-SAFT	2.4970	3.9010	246.60									103
SAFT-VR	2.0560	4.1610	316.00	1.443								53
PC-SAFT	2.6896	3.7729	231.20									55
						Methanol						
soft-SAFT	0.9109	4.0210	214.99		3671.52	52.012						51
SAFT-VR	1.2000	3.5716	200.00	1.797	2275.00	0.32642						97
PC-SAFT	1.5255	3.2300	188.90		2899.50	0.035176						83
						Nitrogen						
BACKONE								1.0471	11.1330	125.74	0.4890	49
SAFT-VR	1.3300	3.1588	81.49	1.550								100
	1.3300	3.1477	73.21	1.599			1.36					100
PC-SAFT	1.2053	3.3130	90.96									55
	1.1400	3.4110	110.10				1.36					88
						Carbon Dioxide						
BACKONE								1.3919	10.5490	291.28	2.1810	49
soft-SAFT	2.6810	2.5340	153.40									102
	1.5710	3.1840	160.20				4.40					102
PC-SAFT	2.0729	2.7852	169.21									55
	2.0420	2.8150	154.01				4.30					88

effect of molecular association, and A^{QQ} represents the Helmholtz free energy due to the quadrupolar−quadrupolar interactions. For pure fluids, the SAFT-type equations studied in this work require three parameters (except for the SAFT-VR approach, which needs four parameters) to describe the number of segments in the model chain and the size and energy of interaction of the segments. Two adjustable parameters are introduced for the representation of associating compounds: the association energy (ϵ^{HB}/k) and the volume available for bonding (k^{HB}). An additional molecular property is needed to characterize the quadrupolar fluids, namely, the quadrupole moment of the molecule (Q), which can be directly applied in the equations as tabulated in the literature. It should be noted that dipolar interactions can also be treated separately by including an additional term in eq 3. As previously mentioned, dipolar molecules are outside the scope of this work.

Blas and Vega[51,52] proposed a modified version of the SAFT[50] approach. The model, named soft-SAFT, incorporates a soft-core LJ potential in the reference fluid and a radial distribution function of LJ spheres in the chain contribution. Within the soft-SAFT approach, molecules are modeled as m tangentially bonded LJ segments of identical diameter σ and dispersive energy ϵ/k. The soft-SAFT model is thus characterized by three molecular parameters for pure fluids: m, σ, and ϵ/k. This approach has been applied to describe thermodynamic properties and phase behavior of alkanes and their mixtures,[51,52] polyethylene,[64] perfluoroalkanes,[65,66] and carbon dioxide.[16,66]

The SAFT-VR approach is a modification of the SAFT[50] equation to deal with different attractive potentials of variable range, such as the square-well, Sutherland, Yukawa, and Mie $m-n$ potentials. The SAFT-VR equation considers molecules to be chains of m tangentially jointed monomeric segments of equal diameter σ interacting through attractive forces modeled by a square-well potential of variable range λ and depth ϵ. Hence, four parameters are required to model a pure fluid: m, σ, λ, and ϵ/k. The SAFT-VR approach has been used to calculate thermodynamic and equilibrium properties for alkanes of low molecular weight and polymers,[53,67,68] their mixtures,[68−73] perfluoroalkanes,[74,75] hydrofluorinated refrigerants,[76,77] and carbon dioxide.[75,78,79]

Gross and Sadowski[55] derived the PC-SAFT EoS by extending the Barker and Henderson perturbation theory to a hard-chain reference fluid. In this model, the chain structure of the molecules is explicitly considered in the dispersion contribution. The PC-SAFT model assumes molecules to be chains formed by m spherical segments of identical diameter σ and characteristic energy ϵ/k. There are three molecular parameters to represent pure substances: m, σ, and ϵ/k. This approach has been used to represent the thermodynamic properties and phase equilibrium behavior of a variety of systems ranging from gases[55] to polymers[80] and copolymers,[81,82] as well as associating[83] and polar[84,85] substances and their mixtures.[86] Several extensions of the PC-SAFT equation to quadrupolar[86−88] fluids have been proposed, mostly derived from results of molecular simulations. In this work, we selected the quadrupolar term proposed by Karakatsani and Economou[88] mainly because of its statistical mechanics basis and the convenient feature that no additional parameters need to be added.

3. Results and Discussion

We tested the capability of the molecular-based equations in predicting third virial coefficients and JTICs for compounds representative of three types of substances: the nonassociating fluids ethane and pentane, the associating fluid methanol, and the quadrupolar fluids carbon dioxide and nitrogen. The molecular parameters for these fluids were taken from the literature, and they are compiled in Table 1 for completeness. It is well-known that analytical EoSs overestimate the critical coordinates because they neglect the long-range density fluctuations that prevail at these conditions. This problem can be overcome by including a crossover treatment[89,90] that describes the universal scaling behavior in the near-critical region and is converted into the original EoS at points well removed from the critical point.

Table 2. Percent Absolute Average Deviation (AAD%) in Predicted Second Virial Coefficients for Selected Compounds from Investigated Molecular Models

EoS	ethane	pentane	methanol[a]	nitrogen[b]	CO_2[b]
BACKONE	4.3	7.4		2.3	8.1
soft-SAFT	12.3	16.6	14.4		17.6
SAFT-VR	40.7	63.7	9.4	12.9	
PC-SAFT	11.0	10.6	13.8	8.7	9.0
T range (K)	245−610	330−655	410−615	138−227	243−487

[a] Modeled including the association term in eq 3. [b] Predicted considering the quadrupolar term in eqs 2 and 3.

However, in this work, we are studying thermodynamic properties away from the critical region. Hence, following usual practice, the experimental critical point[91] was used to scale the temperature and pressure in all cases.

With the objective of evaluating the ability of the molecular models investigated here to represent second virial coefficients, predicted values were compared to the available experimental data.[28] The temperature ranges covered by the experimental values, along with the percent absolute average deviations (AAD%), are reported in Table 2. It can be observed that the lowest deviations are obtained with the BACKONE EoS. This result might be due to the special attention that was devoted to an accurate description of second virial coefficients when the dispersion contribution of the BACKONE model was built,[92] which should improve estimations of this property. At present, we have no explanation for the somewhat poorer performance of the SAFT-VR equation in this respect. A detailed study of the prediction of second virial coefficients is outside the scope of the present work.

3.1. Nonassociating Fluids. We selected two members of the *n*-alkanes series, ethane and pentane, as representative of short and longer nonassociating chain fluids, respectively. Calculations were performed using molecular parameters obtained from the literature (see Table 1). In Figure 1 we show estimated third virial coefficients for ethane from the BACKONE, soft-SAFT, SAFT-VR, and PC-SAFT equations compared to the experimental data available in the literature.[28] In general, good agreement is observed at intermediate temperatures. However, important discrepancies between calculated and experimental values are obtained at low temperatures and around the critical point, where the soft-SAFT, SAFT-VR, and PC-SAFT models predict neither negative values at lower temperatures nor the expected maximum value in the vicinity of the critical temperature; rather, all of them describe an increase toward positive infinity as temperature decreases. This behavior might be due to an inadequate temperature dependence in these models. In addition, as seen in the inset of Figure 1, the soft-SAFT and SAFT-VR models predict a monotonically increasing third virial coefficient at high temperatures, contrary to the expected behavior. This is not the case, however, for the BACKONE EoS predictions, which are in qualitative agreement with experimental values over the entire temperature range. It appears that the particular attention given to second virial coefficients during development of the BACKONE EoS might be acting in favor of a more reliable prediction of third virial coefficients. In this context, Lemmon and Jacobsen[19] recently found that the multiparameter EoSs that describe second virial coefficients well also properly describe third virial coefficients.

Table 3. Percent Absolute Average Deviation (AAD%) in Computed JTIC for Selected Substances from Molecular-Based Models

EoS	ethane	pentane	methanol[a]	nitrogen	CO_2
BACKONE	0.6	0.4	−	5.0	12.8
soft-SAFT	1.5	5.5	11.9	−	28.9,[b]32.0
SAFT-VR	14.9	21.0	8.9	24.0,[b]26.7[c]	−
PC-SAFT	0.8	0.4	11.2	8.3,[b]10.6[c]	15.5,[b]18.4[c]
T range (K)	260−672	399−892	425−810	105−600	127−680

[a] Modeled including the association term in eq 3. [b] Predicted considering the quadrupolar term in eqs 2 and 3. [c] Predicted without considering the quadrupolar term in eqs 2 and 3.

In Figure 2, calculated JTICs for ethane from the BACKONE, soft-SAFT, SAFT-VR, and PC-SAFT equations are depicted

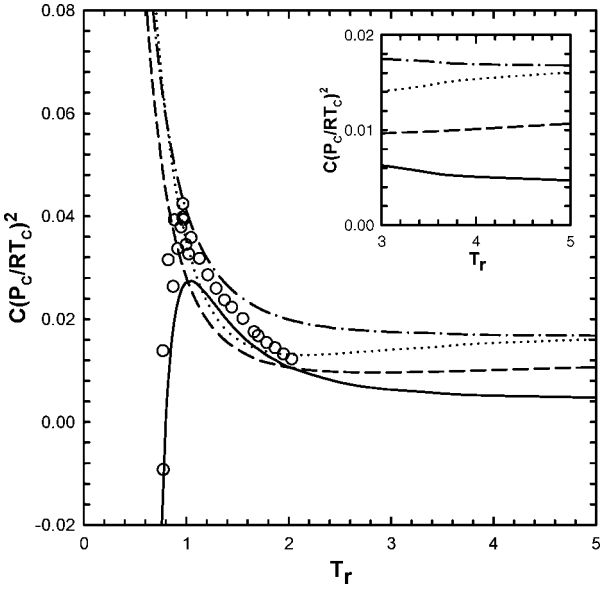

Figure 1. Third virial coefficient for ethane. Comparison of experimental data[28] (symbols) with theoretical results from (solid line) BACKONE EoS, (dotted line) soft-SAFT EoS, (dashed line) SAFT-VR EoS, (dotted-dashed line) PC-SAFT EoS. In the inset, the notation is the same.

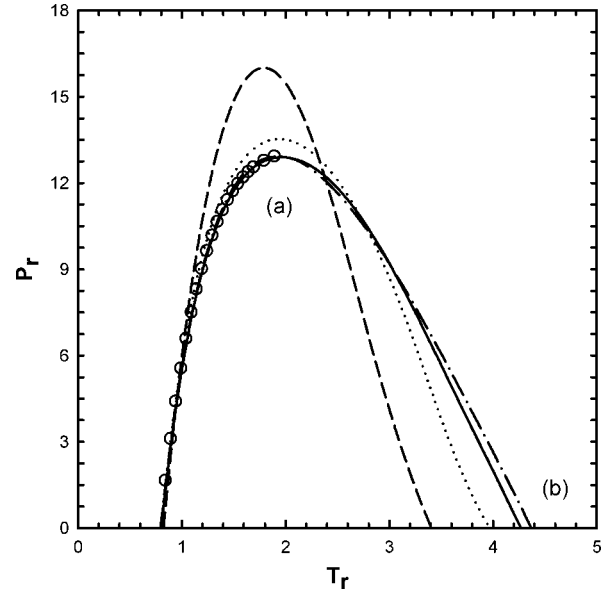

Figure 2. JTIC for ethane. Comparison of experimental data[91] (symbols) with predicted values. The maximum inversion pressure and maximum inversion temperature occur in the regions indicated by a and b, respectively. Notation as in Figure 1.

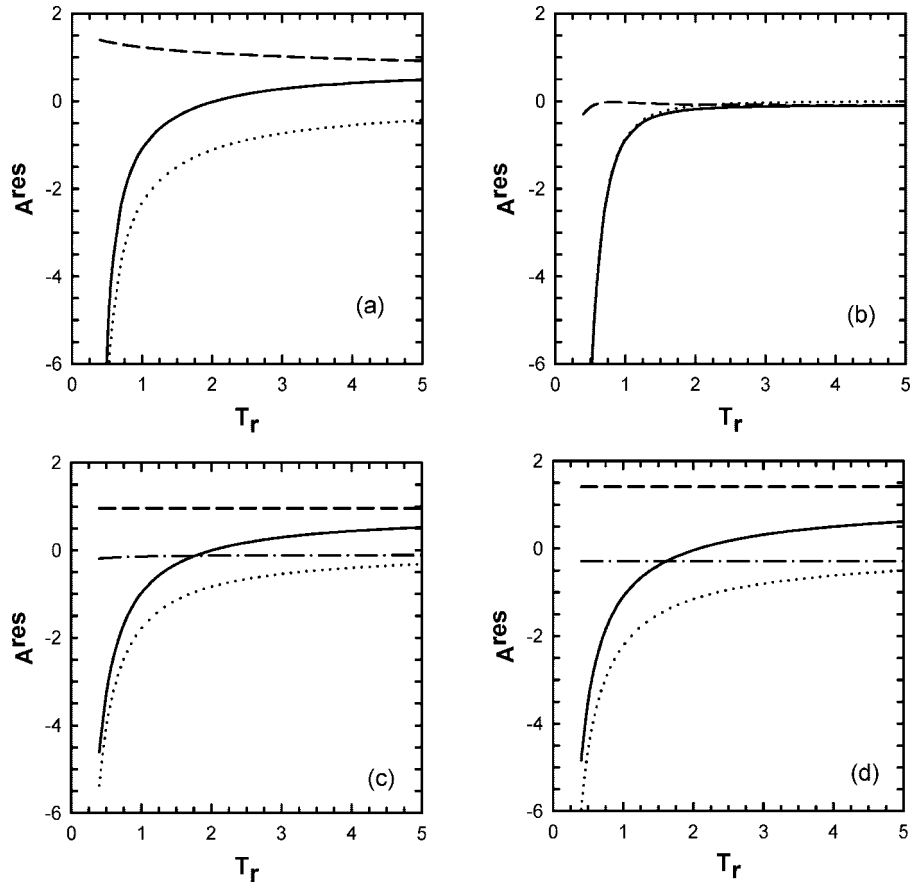

Figure 3. Comparison of the different microscopic contributions to the Helmholtz free energy for ethane at a reduced density of 1.2 as obtained by (a) BACKONE EoS, (b) soft-SAFT EoS, (c) SAFT-VR EoS, (d) PC-SAFT EoS. Solid line, total residual value; dashed line, reference term; dotted line, dispersion term; dashed−dotted line, chain term.

together with the available experimental values.[91] Both the soft-SAFT and SAFT-VR approaches predict a change in curvature of the high-temperature branch when approaching the maximum inversion temperature. This conduct is in contrast to the expected behavior, according to which the course of the JTIC reaches a maximum value and should be smooth and have no further extrema or inflection points in the region of upper temperatures.[93] It can also be seen that the BACKONE and PC-SAFT predictions depict a correctly shaped high-temperature branch because of their adequately estimated third virial coefficients in the region of high temperatures. Table 3 reports the temperature ranges covered by the experimental values along with AAD% values for each model. Taking advantage of the additive structure of eqs 2 and 3, we can compute the separate contributions (e.g., reference, dispersion, chain) to the Helmholtz free energy. Calculations were performed at three values of reduced density: 0.6, 1.2, and 2. In all cases, predictions from the investigated models tended to be very similar. For the sake of clarity in the figures, therefore, only the results at a reduced density of 1.2 are shown for the studied compounds. Figure 3a−d displays results obtained for ethane from the BACKONE, soft-SAFT, SAFT-VR, and PC-SAFT models. It can clearly be seen that the major contribution comes from the dispersion term, which largely dictates the position and shape of the overall energy curve. Hence, the explicit inclusion of the nonspherical molecular shape in the respective dispersion terms of the PC-SAFT and BACKONE models allows an improved representation of dispersive interactions, which might lead to better results for the JTIC and virial coefficients.

To check the performance of selected molecular models on elongated molecules, we present in Figure 4 predicted third virial

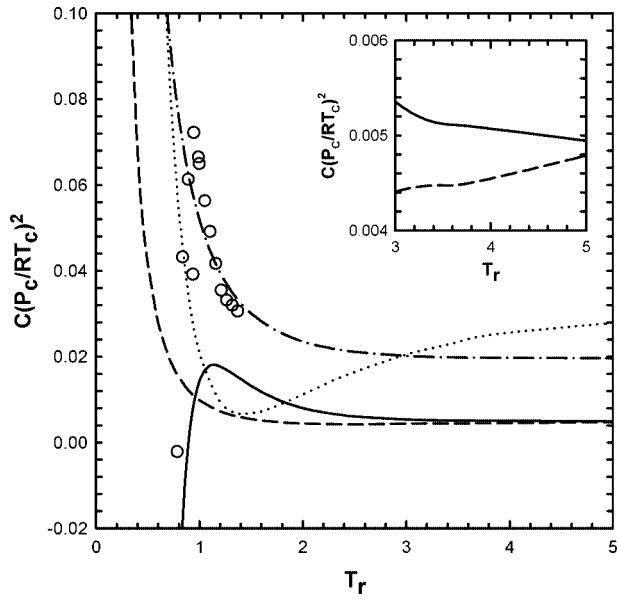

Figure 4. Third virial coefficient for pentane. Comparison of experimental data[28] (symbols) with calculated values. Notation as in Figure 1.

coefficients for pentane from the BACKONE, soft-SAFT, SAFT-VR, and PC-SAFT models along with the available experimental data.[28] It can be seen that the SAFT-type equations fail at describing third virial coefficients at subcritical temperatures, where an adequate temperature dependence from the EoS is needed. It can also be seen that both the soft-SAFT and SAFT-VR predictions show an unrealistic increase of the third virial

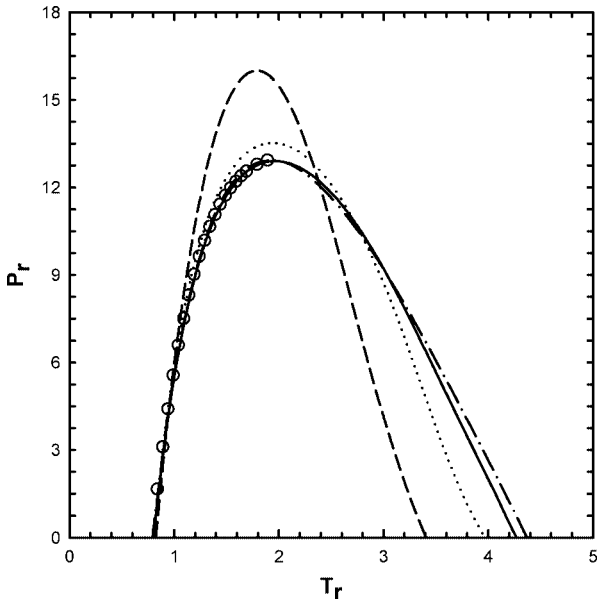

Figure 5. JTIC for pentane. Comparison of experimental data[91] (symbols) with estimated values. Notation as in Figure 1.

coefficient at high temperatures, whereas the BACKONE prediction agrees qualitatively with the experimental data trend.

It has been noticed experimentally that the maximum inversion pressure increases and the maximum inversion temperature decreases with increasing chain length for the members of the same series. The results for pentane are shown in Figure 5, where JTICs estimated by the BACKONE, soft-SAFT, SAFT-VR, and PC-SAFT models are compared to the available experimental data.[91] Both the soft-SAFT and SAFT-VR equations predict a change in curvature of the JTIC near the maximum inversion temperature, which ties in with their erroneous description of third virial coefficients. This is not the case for the PC-SAFT and BACKONE predictions, which display the correct behavior for the whole JTIC. Table 3 contains AAD% values for calculated JTICs from the investigated model. We quantified the different microscopic contributions to the Helmholtz free energy for pentane from the BACKONE, soft-SAFT, SAFT-VR, and PC-SAFT models and present the results in Figure 6a−d. It can clearly be observed that, once again, the dispersion term plays a dominant role. Consequently, the nonsphericity considered in the dispersive interactions by the PC-SAFT and BACKONE approaches can result in better estimations of JTICs and third virial coefficients. On the other hand, it is necessary to mention the marked overestimation of the maximum inversion pressure by the SAFT-VR model, which exceeds 30.83% for ethane and 40.64% for pentane. Bessieres et al.[94] recently reported a similar overestimation when calculating the JTIC for methane using the SAFT-VR approach.

3.2. Associating Fluids. We examined the predictive power of molecular-based models for associating compounds using methanol as an example. Calculations were performed including the association term in eq 3, with molecular parameters available in the literature (see Table 1). The BACKONE EoS was not included in this study because it has no explicit association term. Third virial coefficients of methanol predicted by the soft-SAFT, SAFT-VR, and PC-SAFT models are shown in Figure 7 together with the available experimental data.[28] Calculated values from the IUPAC EoS for methanol[95] are also included. It can be seen that all of the SAFT-type equations correctly describe the decreasing trend at intermediate and high temperatures but fail to capture the experimental behavior at subcritical temperatures (a maximum near the critical temperature and negative values at lower temperatures[28]), where the successful representation of third virial coefficients essentially depends on the built-in temperature dependence of the EoS.

In Figure 8, the JTICs for methanol calculated using the soft-SAFT, SAFT-VR, and PC-SAFT equations are compared to available experimental data.[96] All of the molecular models predicted the correct shape (no inflection points) of the upper-temperature part of the JTIC, reflecting the adequacy of the predicted third virial coefficients at high temperatures. Table 3 reports AAD% values in the calculated JTICs from the investigated models. We evaluated the different contributions to the Helmholtz free energy for methanol from the soft-SAFT, SAFT-VR, and PC-SAFT models. Figure 9a−d presents the results obtained. The clear conclusion to be extracted from this figure is that the association contribution accounts for almost the complete property value. Consequently, the adoption of a particular association scheme can influence the accuracy of predicted properties. In the soft-SAFT and PC-SAFT equations, alkanols are considered to have two association sites (one site on oxygen and one site on hydrogen), whereas in the SAFT-VR approach, alkanols are modeled by using a three-site model (two sites on oxygen and one site on hydrogen), which includes all the association sites present in the methanol molecule. In this context, Clark et al.[97] recently found that phase equilibria and caloric properties of methanol are best represented by SAFT-VR approach using a three-site treatment. Similarly, von Solms et al.[98] showed, based on spectroscopic data, that a three-site model is the most appropriate for methanol.

3.3. Quadrupolar Fluids. We investigated the performance of molecular models when dealing with quadrupolar compounds by using carbon dioxide and nitrogen as examples. Calculations were performed including the quadrupolar term in eqs 2 and 3, with molecular parameters taken from the literature (see Table 1). By taking advantage of the availability of molecular parameters for the models with and without the quadrupolar term, we also studied the influence of the quadrupole moment. Predictions from the SAFT-VR and soft-SAFT models tend to be very similar. For the sake of clarity in the figures, therefore, SAFT-VR results are not shown for carbon dioxide, and soft-SAFT results are not shown for nitrogen. In Figure 10, we show the BACKONE, SAFT-VR, and PC-SAFT predictions for the third virial coefficients of nitrogen, in comparison to the available experimental data.[28] Calculated values from the IUPAC EoS for nitrogen[99] are also included. It can be seen that the SAFT-type equations depict the qualitatively decreasing trend that occurs for intermediate temperatures, except from the original and quadrupolar SAFT-VR approaches, which predict increases at high temperatures. The BACKONE-predicted results are in qualitative agreement with experimental values over all temperature ranges. As expected, the predictions from the quadrupolar versions of SAFT-VR and PC-SAFT are in better agreement with the experimental data than those from the original approaches.

In Figure 11, we display a comparison of the JTICs for nitrogen estimated from the BACKONE, SAFT-VR, and PC-SAFT equations with the available experimental data.[91] As in the previous cases, the predicted behavior of the third virial coefficient has a definite impact on the shape of the JTIC at high temperatures. Thus, the original and quadrupolar SAFT-VR equations predict a change in the JTIC curvature close to the maximum inversion temperature, with the quadrupolar approach being in better agreement with experimental data. The BACKONE, original PC-SAFT, and quadrupolar PC-SAFT

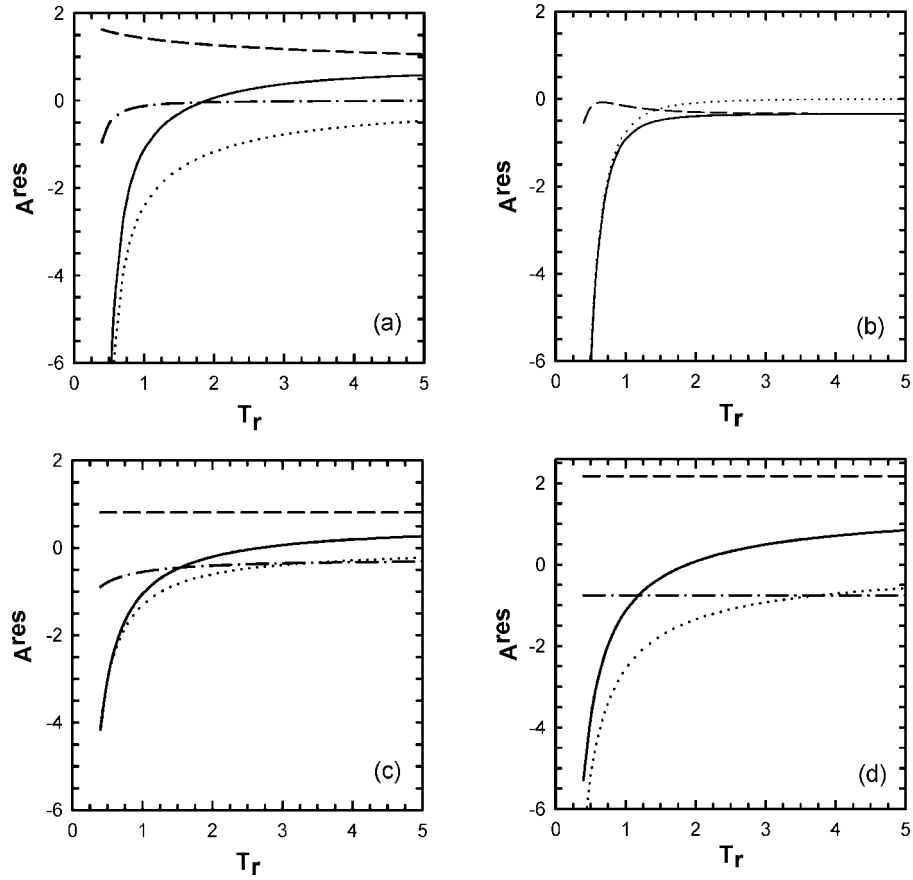

Figure 6. Comparison of the different microscopic contributions to the Helmholtz free energy for pentane at a reduced density of 1.2. Notation as in Figure 3.

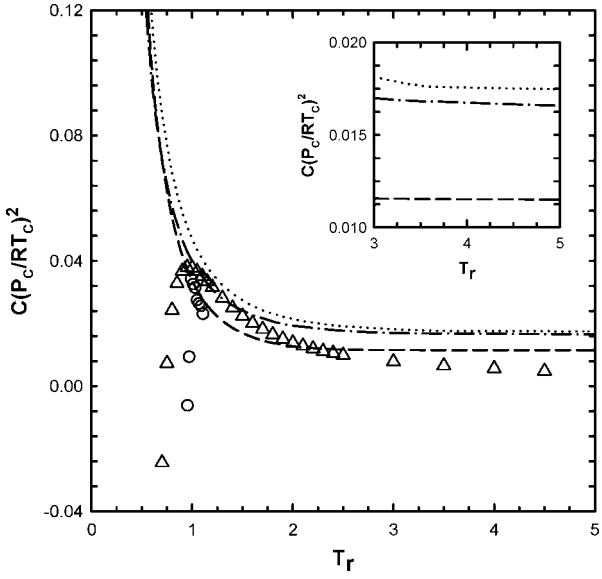

Figure 7. Third virial coefficient for methanol. Open circles, experimental data;[28] open triangles, IUPAC EoS for methanol;[95] dotted line, soft-SAFT EoS; dashed line, SAFT-VR EoS; dotted-dashed line, PC-SAFT EoS. In the inset, the notation is the same.

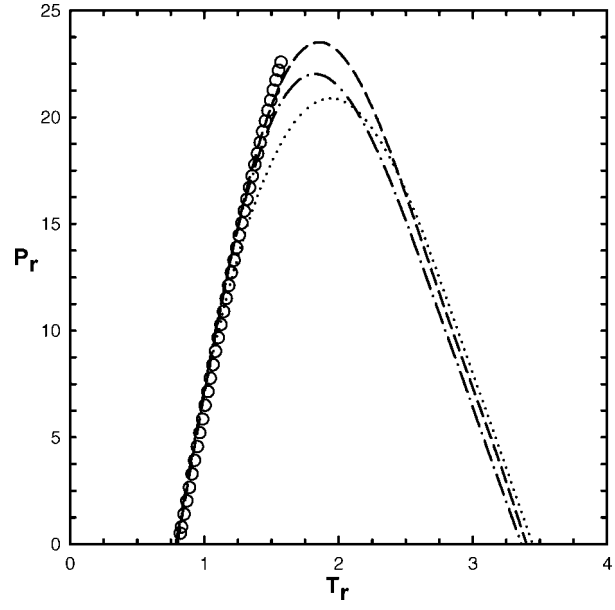

Figure 8. JTIC for methanol. Comparison of experimental data[96] (symbols) with computed values. Notation as in Figure 7.

equations correctly predict the shape of inversion points at high temperatures, with the quadrupolar approach resulting in better agreement with experimental values than the original PC-SAFT. AAD% values with respect to the available experimental data (see Table 3) suggest that the introduction of the quadrupolar contribution does not seem to noticeably influence the description of the JTIC for nitrogen. In this sense, Zhao et al.[100] obtained a slight improvement in the predicted phase behavior for pure nitrogen from the quadrupolar version of SAFT-VR. Similarly, Karakatsani and Economou[88] found that the quadrupole moment of pure nitrogen affects its thermodynamic properties only at subcritical temperatures when using the quadrupolar PC-SAFT approach. A comparison of different microscopic contributions to the Helmholtz free energy for nitrogen from investigated models is shown in Figure 12a−d.

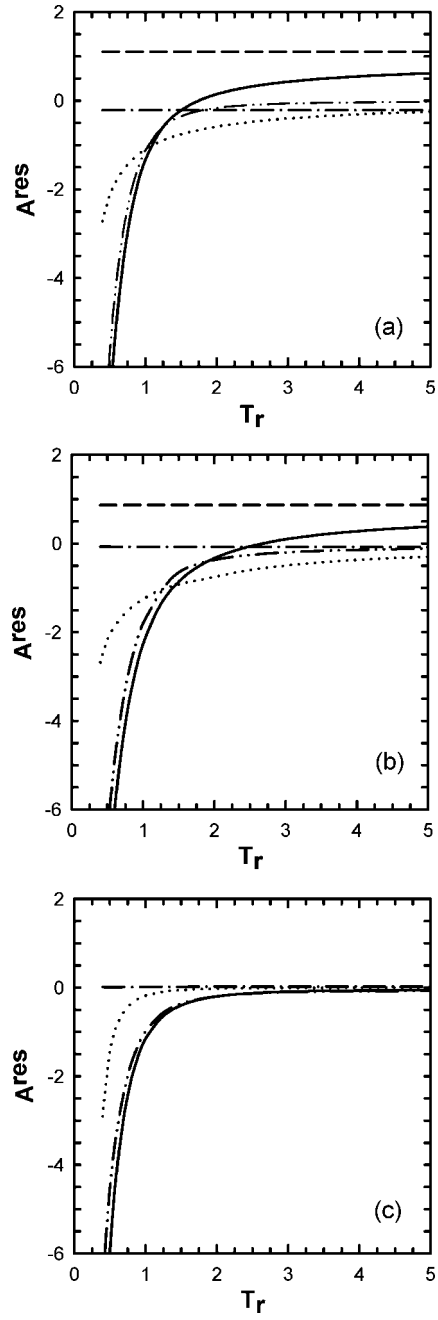

Figure 9. Comparison of the different microscopic contributions to the Helmholtz free energy for methanol at a reduced density of 1.2 as obtained from (a) PC-SAFT EoS, (b) SAFT-VR EoS, (c) soft-SAFT EoS. Solid line, total residual value; dashed line, reference term; dotted line, dispersion term; dashed−dotted line, chain term; dashed−double-dotted line, association term.

It can clearly be seen that dispersion forces are dominant at high temperature. Accordingly, explicitly taking the chain structure of the molecules into account in the dispersion contribution, as is done by the BACKONE and PC-SAFT models, can lead to an enhanced representation of the JTIC and virial coefficients.

Predictions of third virial coefficients for carbon dioxide by the BACKONE, soft-SAFT, and PC-SAFT models are shown in Figure 13 together with the available experimental data.[28] Computed values from the Span−Wagner[101] EoS are also included. It can be seen that the SAFT-types equations predict incorrect values at lower temperatures, and both the original and quadrupolar soft-SAFT models predict increases at high

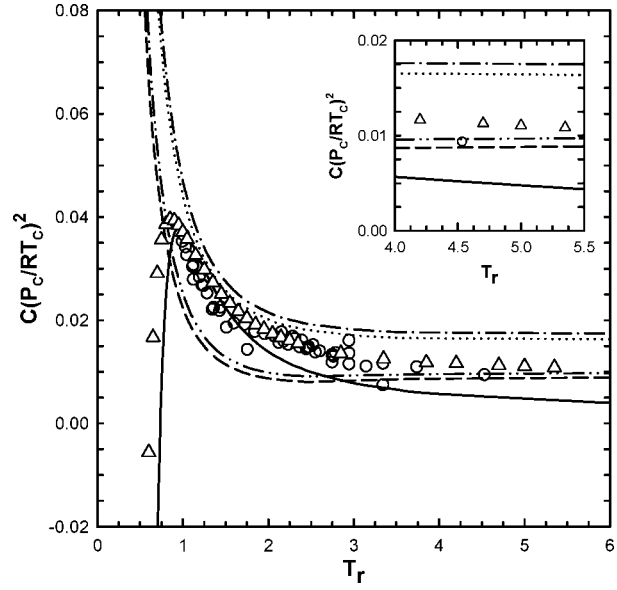

Figure 10. Third virial coefficient for nitrogen. Open circles, experimental data;[28] open triangles, IUPAC EoS for nitrogen;[99] solid line, BACKONE EoS; dotted-dashed line, PC-SAFT EoS; dotted line, quadrupolar PC-SAFT EoS; dashed line, SAFT-VR EoS; dashed−double-dotted line, quadrupolar SAFT-VR EoS. In the inset, the notation is the same.

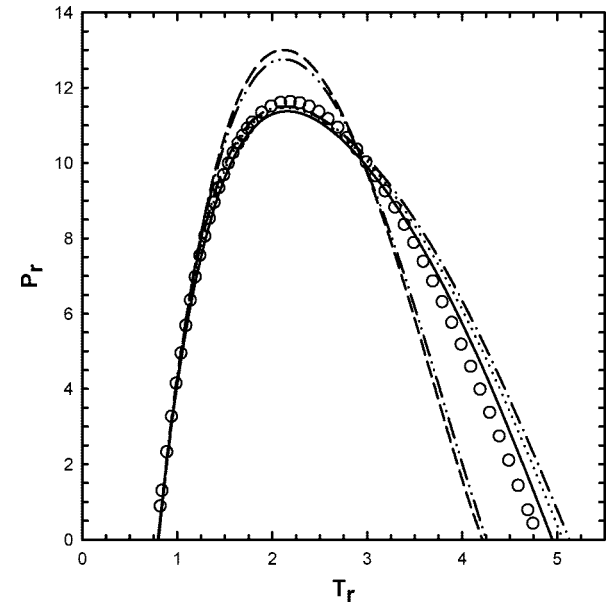

Figure 11. JTIC for nitrogen. Comparison of experimental data[91] (symbols) with calculated values. Notation as in Figure 10.

temperatures. The BACKONE results qualitatively reproduce the experimental trend over the entire range of temperatures. Predicted values from the quadrupolar PC-SAFT equation are in better agreement with the experimental values than those from the original model.

JTICs for carbon dioxide predicted by the the BACKONE, soft-SAFT, and PC-SAFT equations are compared to the available experimental data[91] in Figure 14. It can be seen that the original and quadrupolar soft-SAFT approaches exhibit a noticeable change in curvature of the high-temperature branch close to the maximum inversion temperature, as a result of their incorrectly computed third virial coefficients. The BACKONE and original and quadrupolar PC-SAFT models yield correctly shaped JTICs. The inclusion of the quadrupolar term in the soft-SAFT and PC-SAFT equations leads to better results when

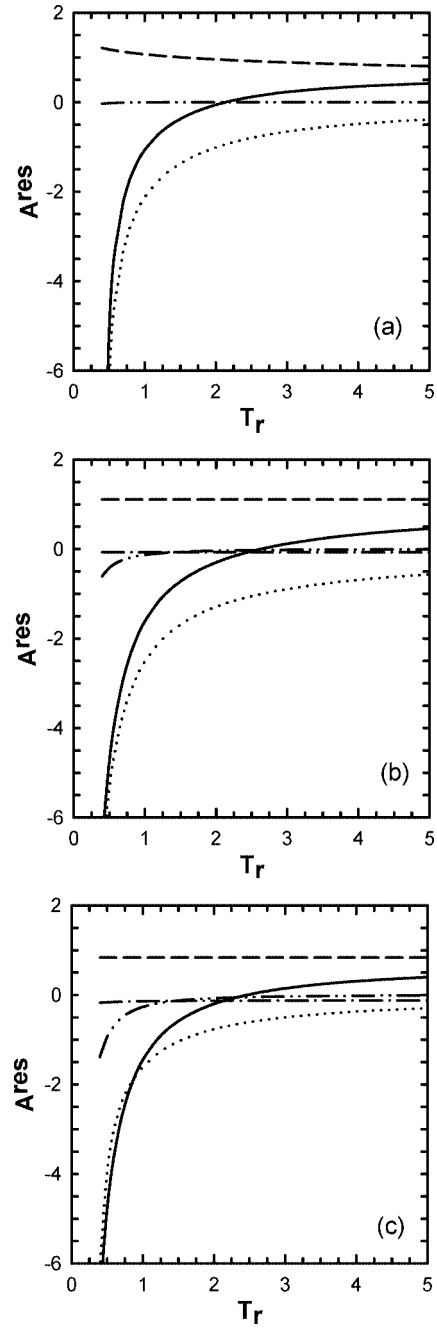

Figure 12. Comparison of the different microscopic contributions to the Helmholtz free energy for nitrogen at a reduced density of 1.2 as obtained by (a) BACKONE EoS, (b) PC-SAFT EoS, (c) SAFT-VR EoS. Solid line, total residual value; dashed line, reference term; dotted line, dispersion term; dashed−dotted line, chain term; dashed−double-dotted line, quadrupolar term.

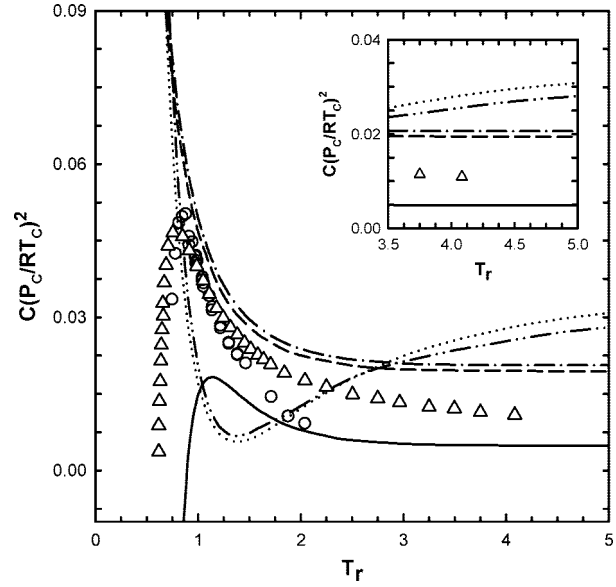

Figure 13. Third virial coefficient for carbon dioxide. Open circles, experimental data;[28] open triangles, Span−Wagner EoS; solid line, BACKONE EoS; dotted-dashed line, PC-SAFT EoS; dashed line, quadrupolar PC-SAFT EoS; dotted line, soft-SAFT EoS; dashed−double-dotted line, quadrupolar soft-SAFT EoS. In the inset, the notation is the same.

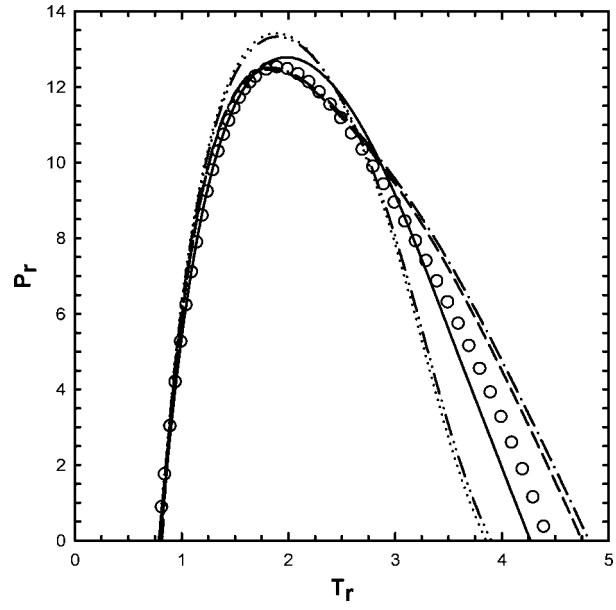

Figure 14. JTIC for carbon dioxide. Comparison of experimental data[91] (symbols) with computed values. Notation as in Figure 13.

compared to those of the original approaches. AAD% values with respect to the available experimental data (see Table 3) appear to suggest that the inclusion of the quadrupole moment has a slight impact on the calculation of the JTIC for carbon dioxide. In a different context, Dias et al.[102] found a relevant influence of the quadrupolar interactions on the prediction of the phase equilibria for mixtures of carbon dioxide and nonaromatic perfluoroalkanes using the quadrupolar soft-SAFT model. A representation of the different molecular contributions to the Helmholtz free energy of carbon dioxide from the studied models is presented in Figure 15a−d. It can clearly be seen that the magnitude of this property is mainly governed by the dispersion contribution. Therefore, the superior performance of the PC-SAFT and BACKONE equations might be due to their respective dispersion terms, which account for the chain-length dependence of the fluid.

4. Conclusions

We have tested the predictive capacity of the BACKONE, soft-SAFT, SAFT-VR, and PC-SAFT models for representing third virial coefficients and JTICs. Calculations were performed for ethane and pentane (nonassociating fluids), methanol (associating fluid), and nitrogen and carbon dioxide (quadrupolar fluids), using the original molecular parameters available in the literature. It was found that the BACKONE EoS outperformed the SAFT-type EoSs in describing second virial coefficients. This result might be due to the special attention that was devoted to an accurate representation of second virial coefficients in the

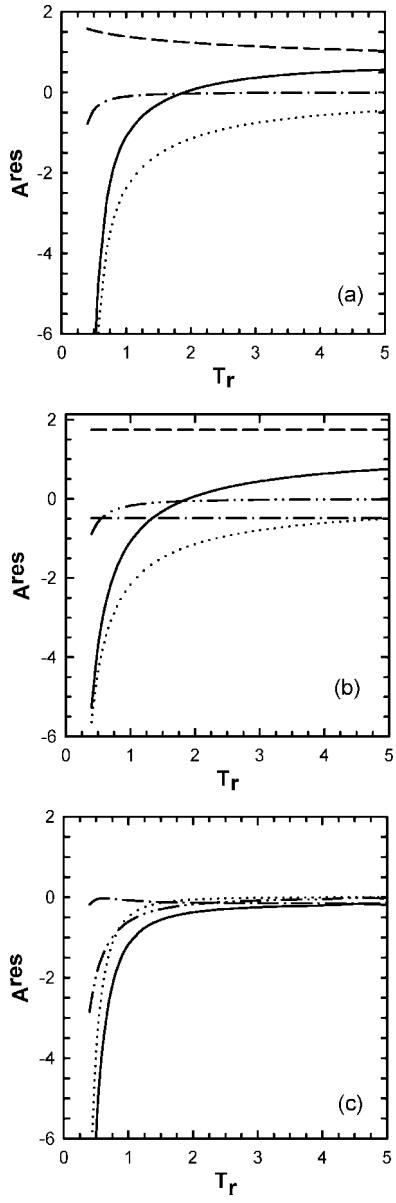

Figure 15. Comparison of the different microscopic contributions to the Helmholtz free energy for carbon dioxide at a reduced density of 1.2 as obtained by (a) BACKONE EoS, (b) PC-SAFT EoS, (c) soft-SAFT EoS. Solid line, total residual value; dashed line, reference term; dotted line, dispersion term; dashed−dotted line, chain term; dashed−double-dotted line, quadrupolar term.

development of the BACKONE model. By taking advantage of the molecular nature of the studied models, we separately quantified the several microscopic contributions to the Helmholtz free energy. We found that, for both nonassociating and quadrupolar compounds, the major contribution comes from the dispersion term, whereas associating fluids are mainly governed by the association contribution. In this context, the explicit inclusion of the nonspherical molecular shape in dispersion terms by the PC-SAFT and BACKONE models leads to better estimations of third virial coefficients and JTICs for nonassociating and quadrupolar fluids. The use of an associating three-site scheme was found to be in better agreement with experimental data for methanol. We validated our previous findings that the deterioration in the shape of the computed JTIC at high temperatures indicates the inadequacy of predicted third virial coefficients. Accordingly, much care should be paid to the reliable representation of virial coefficients in the development of any new EoS.

Literature Cited

(1) Kortekaas, W. G.; Peters, C. J.; de Swaan Arons, J. Joule−Thomson Expansion of High-Pressure−High-Temperature Gas Condensates. *Fluid Phase Equilib.* **1997**, *139*, 205.

(2) Amara, M.; Capatina-Papaghiuc, D.; Denel, B.; Terpolilli, P. Mixed Finite Element Approximation for a Coupled Petroleum Reservoir Model. *ESAIM Math. Model. Numer. Anal.* **2005**, *39* (2), 349.

(3) Colina, C. M.; Müller, E. A. Joule−Thomson Inversion Curves by Molecular Simulation. *Mol. Sim.* **1997**, *19*, 237.

(4) Colina, C. M.; Müller, E. A. Molecular Simulation of Joule−Thomson Inversion Curves. *Int. J. Thermophys.* **1999**, *20* (1), 229.

(5) Chacín, A.; Vasquez, J. M.; Müller, E. A. Molecular Simulation of the Joule−Thomson Inversion Curve of Carbon Dioxide. *Fluid Phase Equilib.* **1999**, *165*, 147.

(6) Colina, C. M.; Lisal, M.; Siperstein, F. R.; Gubbins, K. E. Accurate CO_2 Joule−Thomson Inversion Curve by Molecular Simulations. *Fluid Phase Equilib.* **2002**, *202*, 253.

(7) Colina, C. M.; Olivera-Fuentes, C. G.; Siperstein, F. R.; Lisal, M.; Gubbins, K. E. Thermal Properties of Supercritical Carbon Dioxide by Monte Carlo Simulations. *Mol. Sim.* **2003**, *29* (6−7), 405.

(8) Lagache, M. H.; Ungerer, Ph.; Boutin, A.; Fuchs, A. H. Prediction of Thermodynamic Derivative Properties of Natural Condensate Gases at High Pressure by Monte Carlo Simulation. *Phys. Chem. Chem. Phys.* **2001**, *3*, 4333.

(9) Escobedo, F. A.; Chen, Z. Simulation of Isoenthalps and Joule−Thomson Inversion Curves of Pure Fluids and Mixtures. *Mol. Sim.* **2001**, *26* (6), 395.

(10) Escobedo, F. A. A Unified Methodological Framework for the Simulation of Nonisothermal Ensembles. *J. Chem. Phys.* **2005**, *123*, 044110.

(11) Lagache, M. H. Prediction of Thermodynamic Derivative Properties of Natural Condensate Gases at High Pressure by Monte Carlo Simulation. *Fluid Phase Equilib.* **2004**, *220*, 211.

(12) Lisal, M.; Smith, W. R.; Aim, K. Direct Molecular-Level Monte Carlo Simulation of Joule−Thomson Processes. *Mol. Phys.* **2003**, *101* (18), 2875.

(13) Kristof, T.; Rutkai, G.; Laszlo, M.; Liszi, J. Molecular Simulation of the Joule−Thomson Inversion Curve of Hydrogen Sulphide. *Mol. Phys.* **2005**, *103* (4), 537.

(14) Miller, D. Joule−Thomson Inversion Curve, Corresponding States, and Simpler Equations of State. *Ind. Eng. Chem. Fundam.* **1970**, *9*, 585.

(15) Nichita, D. V.; Leibovici, C. F. Calculation of Joule−Thomson Inversion Curves for Two-Phase Mixtures. *Fluid Phase Equilib.* **2006**, *246*, 167.

(16) Colina, C. M.; Turrens, L. F.; Gubbins, K. E.; Olivera-Fuentes, C. G.; Vega, L. F. Predictions of the Joule−Thomson Inversion Curve for the *n*-Alkane Series and Carbon Dioxide from the Soft-SAFT Equation of State. *Ind. Eng. Chem. Res.* **2002**, *41*, 1069.

(17) Colina, C. M.; Olivera-Fuentes, C. G. Predicted Inversion Curve and Third Virial Coefficients of Carbon Dioxide at High Temperatures. *Ind. Eng. Chem. Res.* **2002**, *41*, 1064.

(18) Pitzer, K. S.; Sterner, S. M. Equations of State Valid Continuously from Zero to Extreme Pressures for H_2O and CO_2. *J. Chem. Phys.* **1994**, *101* (4), 3111.

(19) Lemmon, E. W.; Jacobsen, R. T. A New Functional Form and New Fitting Techniques for Equations of State with Application to Pentafluoroethane (HFC-125). *J. Phys. Chem. Ref. Data* **2005**, *34* (1), 69.

(20) Chirico, R.; Steel, W. V. Reconciliation of Calorimetrically and Spectroscopically Derived Thermodynamic Properties at Pressures Greater Than 0.1 MPa for Benzene and Methylbenzene: The Importance of the Third Virial Coefficient. *Ind. Eng. Chem. Res.* **1994**, *33*, 157.

(21) Steel, W. V.; Chirico, R. D.; Nguyen, A.; Knipmeyer, S. E. Vapor Pressures, High-Temperature Heat Capacities, Critical Properties, Derived Thermodynamic Functions, and Barriers to Methyl-Group Rotation, for the Six Dimethylpyridines. *J. Chem. Thermodyn.* **1995**, *27*, 311.

(22) Chirico, R. D.; Klots, T. D.; Knipmeyer, S. E.; Nguyen, A.; Steel, W. V. Reconciliation of Calorimetrically and Spectroscopically Derived Standard Entropies for the Six Dimethylpyridines Between the Temperatures 250K and 650 K: A Stringent Test of Thermodynamic Consistency. *J. Chem. Thermodyn.* **1998**, *30*, 535.

(23) Ichikura, K.; Kano, Y.; Sato, H. Importance of Third Virial Coefficients for Representing the Gaseous Phase Based on Measuring PVT Properties of 1,1,1,-Trifluoroethane (R143a). *Int. J. Thermophys.* **2006**, *27* (1), 23.

(24) Boublik, T. Equilibrium Behaviour of Fluids in the Critical Region from the Fourth-Order Virial Expansion Supercritical Fluid Extraction of Solids. *Fluid Phase Equilib.* **2001**, *182*, 47.

(25) Tomberli, B.; Goldman, S.; Gray, C. G. Predicting Solubility in Supercritical Solvents Using Estimated Virial Coefficients and Fluctuation Theory. *Fluid Phase Equilib.* **2001**, *187*−*188*, 111.

(26) Saldaña, M. D.; Tomberli, B.; Guigard, S. E.; Goldman, S.; Gray, C. G.; Temelli, F. Determination of Vapor Pressure and Solubility Correlation of Phenolic Compounds in Supercritical CO_2. *J. Supercrit. Fluids* **2007**, *40*, 7.

(27) Gliko, O.; Pan, W.; Katsonis, P.; Neumaier, N.; Galkin, O.; Weinkauf, S.; Vekilov, P. Metastable Liquid Clusters in Super- and Undersaturated Protein Solutions. *J. Phys. Chem. B* **2007**, *111*, 3106.

(28) Dymond, J. H.; Marsk, K. N.; Wilhoit, R. C.; Wong, K. C. *Landolt*−*Börnstein Numerical Data and Functional Relationships in Science and Technology, Group IV*; Springer: New York, 2002; Vol. 21A.

(29) Goodwin, A. R.; Moldover, M. R. Methanol Thermodynamic Properties from 176 to 673K at Pressures to 700 bar. *J. Chem. Phys.* **1990**, *93*, 2741.

(30) Boyes, S. J.; Weber, L. A. Vapour Pressures and Gas-Phase (p, ρn, T) Values for CF_3CHF_2 (R125). *J. Chem. Thermodyn.* **1995**, *27*, 163.

(31) Gillis, K. A. Thermodynamic Properties of Seven Gaseous Halogenated Hydrocarbons from Acoustic Measurements: $CHClFCF_3$, CHF_2CF_3, CF_3CH_3, CHF_2CH_3, $CF_3CHFCHF_2$, $CF_3CH_2CF_3$, and $CHF_2CF_2CH_2F$. *Int. J. Thermophys* **1997**, *18*, 73.

(32) Speedy, R. Third Virial Coefficients for Saturated Square Well Particles. *J. Chem. Phys.* **1997**, *106* (23), 9793.

(33) Vega, C.; Saager, B.; Fischer, J. Molecular Dynamics Studies for the New Refrigerant R152a with Simple Model Potentials. *Mol. Phys.* **1989**, *68*, 1079.

(34) Kohler, F.; Nguyen Van, N. The Second Virial Coefficients of Some Halogenated Ethanes. *Mol. Phys.* **1993**, *80*, 795.

(35) Vega, C.; McBride, C.; Menduina, C. The Second Virial Coefficient of the Dipolar Two Center Lennard-Jones Model. *Phys. Chem. Chem. Phys.* **2002**, *4*, 3000.

(36) Moller, D.; Fischer, J. Determination of an Effective Intermolecular Potential for Carbon Dioxide Using Vapor−Liquid Phase Equilibria from NPT Plus Test Particle Simulations. *Fluid Phase Equilib.* **1994**, *100*, 35.

(37) Vrabec, J.; Stoll, J.; Hasse, H. A Set of Molecular Models for Symmetric Quadrupolar Fluids. *J. Phys. Chem. B* **2001**, *105*, 12126.

(38) Menduina, C.; McBride, C.; Vega, C. The Second Virial Coefficient of Quadrupolar Two Center Lennard-Jones Models. *Phys. Chem. Chem. Phys.* **2001**, *3*, 1289.

(39) MacDowell, L. G.; Menduina, C.; Vega, C.; de Miguel, E. Third Virial Coefficients and Critical Properties of Quadrupolar Two Center Lennard-Jones Models. *Phys. Chem. Chem. Phys.* **2003**, *5*, 2851.

(40) MacDowell, L. G.; Menduina, C.; Vega, C.; de Miguel, E. Critical Properties of Molecular Fluids from the Virial Series. *J. Chem. Phys.* **2003**, *119*, 11367.

(41) De Santis, R.; Grande, B. An Equation for Predicting Third Virial Coefficients of Nonpolar Gases. *AIChE J.* **1979**, *25* (6), 931.

(42) Orbey, H.; Vera, J. H. Correlation for the Third Virial Coefficient Using T_c, P_c and ω as Parameters. *AIChE J.* **1983**, *29* (1), 107.

(43) Bosse, M. A.; Reich, R. Correlation for the Third Virial Coefficient Using T_c, P_c, Dipolar Polarizability and Mean Radius of Gyration as Parameters. *Chem. Eng. Commun.* **1988**, *66*, 83.

(44) Liu, D. X.; Xiang, H. W. Corresponding-States Correlation and Prediction of Third Virial Coefficients for a Wide Range of Substances. *Int. J. Thermophys.* **2003**, *24* (6), 1667.

(45) Meng, L.; Duan, Y.; Li, L. Correlations for Second and Third Virial Coefficients of Pure Fluids. *Fluid Phase Equilib.* **2004**, *226*, 109.

(46) Weber, L. A. Estimating the Virial Coefficients of Small Polar Molecules. *Int. J. Thermophys.* **1994**, *15*, 461.

(47) Van Nhu, N.; Iglesias-Silva, G. A.; Kohler, F. Correlation of Third Virial Coefficients to Second Virial Coefficients. *Ber. Bunsen-Ges. Phys. Chem.* **1989**, *93*, 526.

(48) Ramos-Estrada, M.; Iglesias-Silva, G. A.; Hall, K. R.; Kohler, F. Estimation of Third Virial Coefficients at Low Reduced Temperatures. *Fluid Phase Equilib.* **2006**, *240*, 179.

(49) Weingerl, U.; Wendland, M.; Fischer, J.; Müller, A.; Winkelmann, J. Backone Family of Equations of State: 2. Nonpolar and Polar Fluid Mixtures. *AIChE J.* **2001**, *47* (3), 705.

(50) Chapman, W. G.; Jackson, G.; Gubbins, K. E. Phase Equilibria of Associating Fluids: Chain Molecules with Multiple Bonding Sites. *Mol. Phys.* **1988**, *65*, 1057.

(51) Blas, F. J.; Vega, L. F. Prediction of Binary and Ternary Diagrams Using the Statistical Associating Fluid Theory (SAFT) Equation of State. *Ind. Eng. Chem. Res.* **1998**, *37*, 660.

(52) Blas, F. J.; Vega, L. F. Critical Behavior and Partial Miscibility Phenomena in Binary Mixtures of Hydrocarbons by the Statistical Associating Fluid Theory. *J. Chem. Phys.* **1998**, *109* (17), 7405.

(53) Gil-Villegas, A.; Galindo, A.; Whitehead, P. J.; Mills, S. L.; Jackson, G.; Burgess, A. N. Statistical Associating Fluid Theory for Chain Molecules with Attractive Potentials of Variable Range. *J. Chem. Phys.* **1997**, *106* (10), 4168.

(54) Galindo, A.; Davies, L. A.; Gil-Villegas, A.; Jackson, G. The Thermodynamics of Mixtures and the Corresponding Mixing Rules in the SAFT-VR Approach for Potentials of Variable Range. *Mol. Phys.* **1998**, *93* (2), 241.

(55) Gross, J.; Sadoswki, G. Perturbed-Chain SAFT: An Equation of State Based on a Perturbation Theory for Chain Molecules. *Ind. Eng. Chem. Res.* **2001**, *40*, 1244.

(56) Müller, E. A.; Gubbins, K. E. Molecular-Based Equations of State for Associating Fluids: A Review of SAFT and Related Approaches. *Ind. Eng. Chem. Res.* **2001**, *40*, 2193.

(57) Wei, Y. S.; Sadus, R. Equations of State for the Calculation of Fluid-Phase Equilibria. *AIChE J.* **2000**, *46* (1), 169.

(58) Economou, I. G. Statistical Associating Fluid Theory: A Successful Model for the Calculation of Thermodynamic and Phase Equilibrium Properties of Complex Fluid Mixtures. *Ind. Eng. Chem. Res.* **2002**, *41*, 953.

(59) Chen, S. S.; Kreglewski, A. Application of the Augmented van der Waals Theory of Fluids: I. Pure Fluids. *Ber. Bunsen-Ges. Phys. Chem* **1977**, *81*, 1048.

(60) Müller, A.; Winkelman, J.; Fischer, J. Backone Family of Equations of State: 1. Nonpolar and Polar Pure Fluids. *AIChE J.* **1996**, *42* (4), 1116.

(61) Calero, S.; Wendland, M.; Fischer, J. Description of alternative refrigerants with BACKONE equations. *Fluid Phase Equilib.* **1998**, *152*, 1.

(62) Weingerl, U.; Fischer, J. Consideration of dipole−quadrupole interactions in molecular based equations of state. *Fluid Phase Equilib.* **2002**, *202*, 49.

(63) Wendland, M.; Saleh, B.; Fischer, J. Accurate Thermodynamic Properties from the BACKONE Equation for the Processing of Natural Gas. *Energy & Fuels.* **2004**, *18* (4), 938.

(64) Pedrosa, N.; Vega, L. F.; Coutinho, J. A. P.; Marrucho, I. M. Phase Equilibria Calculations of Polyethylene Solutions from SAFT-Type Equations of State. *Macromolecules* **2006**, *39*, 4240.

(65) Dias, A. M.A.; Pamies, J. C.; Coutinho, J. A. P.; Marrucho, I. M.; Vega, L. F. SAFT Modeling of the Solubility of Gases in Perfluoroalkanes. *J. Phys. Chem. B* **2004**, *108*, 1450.

(66) Dias, A. M.A.; Carrier, H.; Daridon, J. L.; Pamies, J. C.; Vega, L. F.; Coutinho, J. A. P.; Marrucho, I. M. Vapor−Liquid Equilibrium of Carbon Dioxide−Perfluoroalkane Mixtures: Experimental Data and SAFT Modeling. *Ind. Eng. Chem. Res.* **2006**, *45*, 2341.

(67) McCabe, C.; Jackson, G. SAFT-VR Modelling of the Phase Equilibrium of Long-Chain *n*-Alkanes. *Phys. Chem. Chem. Phys.* **1999**, *1*, 2057.

(68) McCabe, C.; Gil-Villegas, A.; Jackson, G. Predicting the High-Pressure Phase Equilibria of Methane + *n*-Hexane Using the SAFT-VR Approach. *J. Phys. Chem. B* **1998**, *102*, 4183.

(69) Filipe, E. J. M.; de Azevedo, E.; Martins, L. F. G.; Soares, V. A. M.; Calado, J. C. G.; McCabe, C.; Jackson, G. Thermodynamics of Liquid Mixtures of Xenon with Alkanes: (Xenon + Ethane) and (Xenon + Propane). *J. Phys. Chem. B* **2000**, *104*, 1315.

(70) Filipe, E. J. M.; Martins, L. F. G.; Calado, J. C. G.; McCabe, C.; Jackson, G. Thermodynamics of Liquid Mixtures of Xenon with Alkanes: (Xenon + *n*-Butane) and (Xenon + Isobutane). *J. Phys. Chem. B* **2000**, *104*, 1322.

(71) Sun, L. X.; Zhao, H. G.; Kiselev, S. B.; McCabe, C. Predicting Mixture Phase Equilibria and Critical Behavior Using the SAFT-VRX Approach. *J. Phys. Chem. B* **2005**, *109*, 9047.

(72) Dias, L. M. B.; Filipe, E. J. M.; Calado, J. C. G.; McCabe, C. Thermodynamics of Liquid (Xenon + Methane) Mixtures. *J. Phys. Chem. B* **2004**, *108*, 7377.

(73) McCabe, C.; Galindo, A.; Garcia-Lisbona, M. N.; Jackson, G. Examining the Adsorption (Vapor−Liquid Equilibria) of Short-Chain Hydrocarbons in Low-Density Polyethylene with the SAFT-VR Approach. *Ind. Eng. Chem. Res.* **2001**, *40*, 3835.

(74) McCabe, C.; Galindo, A.; Gil-Villegas, A.; Jackson, G. Predicting the High-Pressure Phase Equilibria of Binary Mixtures of Perfluoro-*n*-Alkanes plus *n*-Alkanes Using the SAFT-VR Approach. *J. Phys. Chem. B* **1998**, *102*, 8060.

(75) Colina, C. M.; Gubbins, K. E. Vapor−Liquid and Vapor−Liquid−Liquid Equilibria of Carbon Dioxide/*n*-Perfluoroalkane/*n*-Alkane Ternary Mixtures. *J. Phys. Chem. B* **2005**, *109*, 2899.

(76) Galindo, A.; Gil-Villegas, A.; Whitehead, P. J.; Jackson, G.; Burgess, A. N. Prediction of Phase Equilibria for Refrigerant Mixtures of Difluoromethane (HFC-32), 1,1,1,2-Tetrafluoroethane (HFC-134a), and Pentafluoroethane (HFC-125a) Using SAFT-VR. *J. Phys. Chem. B* **1998**, *102*, 7632.

(77) Swaminathan, S.; Visco, D. P. Thermodynamic Modeling of Refrigerants Using the Statistical Associating Fluid Theory with Variable Range. 1. Pure Components. *Ind. Eng. Chem. Res.* **2005**, *44*, 4798.

(78) Galindo, A.; Blas, F. L. J. Theoretical Examination of the Global Fluid Phase Behavior and Critical Phenomena in Carbon Dioxide + *n*-Alkane Binary Mixtures. *J. Phys. Chem. B* **2002**, *106*, 4503.

(79) Blas, F. L.; Galindo, A. Study of the High Pressure Phase Behaviour of CO_2 + *n*-Alkane Mixtures Using the SAFT-VR Approach with Transferable Parameters. *Fluid Phase Equilib.* **2002**, *194*−*197*, 501.

(80) Gross, J.; Sadoswki, G. Modeling Polymer Systems Using the Perturbed-Chain Statistical Associating Fluid Theory Equation of State. *Ind. Eng. Chem. Res.* **2002**, *41*, 1084.

(81) Gross, J.; Spuhl, O.; Tumakaka, F.; Sadoswki, G. Modeling Copolymer Systems Using the Perturbed-Chain SAFT Equation of State. *Ind. Eng. Chem. Res.* **2003**, *42*, 1266.

(82) Becker, F.; Buback, M.; Latz, H.; Sadoswki, G.; Tumakaka, F. Cloud-Point Curves of Ethylene−(Meth)acrylate Copolymers in Fluid Ethene up to High Pressures and Temperatures: Experimental Study and PC-SAFT Modeling. *Fluid Phase Equilib.* **2004**, *215*, 263.

(83) Gross, J.; Sadoswki, G. Application of the Perturbed-Chain SAFT Equation of State to Associating Systems. *Ind. Eng. Chem. Res.* **2002**, *41*, 5510.

(84) Tumakaka, F.; Sadoswki, G. Application of the Perturbed-Chain SAFT Equation of State to Polar Systems. *Fluid Phase Equilib.* **2004**, *217*, 233.

(85) Dominik, A.; Chapman, W. G.; Kleiner, M.; Sadowski, G. Modeling of Polar Systems with the Perturbed-Chain SAFT Equation of State. Investigation of the Performance of Two Polar Terms. *Ind. Eng. Chem. Res.* **2005**, *44*, 6928.

(86) Tumakaka, F.; Gross, J.; Sadoswki, G. Thermodynamic Modeling of Complex Systems Using PC-SAFT. *Fluid Phase Equilib.* **2005**, *228*−*229*, 89.

(87) Gross, J. An Equation-of-State Contribution for Polar Components: Quadrupolar Molecules. *AIChE J.* **2005**, *51* (9), 2556.

(88) Karakatsani, E. K.; Economou, I. G. Perturbed Chain-Statistical Associating Fluid Theory Extended to Dipolar and Quadrupolar Molecular Fluids. *J. Phys. Chem. B* **2006**, *110*, 9252.

(89) Kiselev, S. B.; Ely, J. F. Crossover SAFT Equation of State: Application for Normal Alkanes. *Ind. Eng. Chem. Res.* **1999**, *38*, 4993.

(90) McCabe, C.; Kiselev, S. B. Application of Crossover Theory to the SAFT-VR Equation of State: SAFT-VRX for Pure Fluids. *Ind. Eng. Chem. Res.* **2004**, *43*, 2839.

(91) Lemmon, E. W.; McLinden, M. O.; Friend, D. G. Thermophysical properties of fluid systems. In *NIST Chemistry WebBook, NIST Standard Reference Database Number 69*; Linstrom, P. J., Mallard, W. G., Eds.; National Institute of Standards and Technology (NIST): Gaithersburg, MD, 2005; available at http://webbook.nist.gov/chemistry/. (accessed June 2007).

(92) Mecke, M.; Müller, A.; Winkelman, J.; Fischer, J. An Equation of State for Two-Center Lennard-Jones Fluids. *Int. J. Thermophys.* **1997**, *18* (3), 683.

(93) Deiters, U K; De Reuck, K. M. Guidelines for Publication of Equations of State I. Pure Fluids. *Fluid Phase Equilib.* **1999**, *161*, 205.

(94) Bessieres, D.; Randzio, S. L.; Piñeiro, M. M.; Lafitte, Th.; Daridon, J-L. A Combined Pressure-Controlled Scanning Calorimetry and Monte Carlo Determination of the Joule−Thomson Inversion Curve. Application to Methane. *J. Phys. Chem. B* **2006**, *110*, 5659.

(95) de Reuck, K. M., Craven, R. J. B., Eds. *Methanol*; International Thermodynamic Tables of the Fluid State; IUPAC/Blackwell Scientific: Oxford, U.K., 1993; Vol. 12.

(96) Goodwin, R. D. Methanol Thermodynamic Properties form 176 to 673 K at pressures to 700 bar. *J. Phys. Chem. Ref. Data* **1987**, *16*, 799.

(97) Clark, G.; Haslam, A.; Galindo, A.; Jackson, G. Developing Optimal Wertheim-Like Models of Water for Use in Statistical Associating Fluid Theory (SAFT) and Related Approaches. *Mol. Phys.* **2006**, *104* (22−24), 3561.

(98) von Solms, N.; Michelsen, M. L.; Pereira, C.; Derawi, S. O.; Kontogeorgis, G. M. Investigating Models for Associating Fluids Using Spectroscopy. *Ind. Eng. Chem. Res.* **2006**, *45*, 5368.

(99) Angus, S.; Armstrong, B.; de Reuck, K. *Nitrogen*; International Thermodynamic Tables of the Fluid State; IUPAC/Blackwell Scientific: Oxford, U.K., 1993; Vol. 6.

(100) Zhao, H.; Morgado, P.; Gil-Villegas, A.; McCabe, C. Predicting the Phase Behavior of Nitrogen + *n*-Alkanes for Enhanced Oil Recovery from the SAFT-VR Approach: Examining the Effect of the Quadrupole Moment. *J. Phys. Chem. B* **2006**, *110*, 24083.

(101) Span, R.; Wagner, W. A New Equation of State for Carbon Dioxide Covering the Fluid Region from the Triple-Point Temperature to 1100 K at Pressures up to 800 MPa. *J. Phys. Ref. Data* **1996**, *25* (6), 1509.

(102) Dias, A.; Carrier, H.; Daridon, J.; Pamies, J.; Vega, L.; Coutinho, J.; Marrucho, M. Vapor−Liquid Equilibrium of Carbon Dioxide−Perfluoroalkane Mixtures: Experimental Data and SAFT Modeling. *Ind. Eng. Chem. Res.* **2006**, *45*, 2341.

(103) Pamies, J.; Vega, L. F. Vapor−Liquid Equilibria and Critical Behavior of Heavy *n*-Alkanes Using Transferable Parameters from the Soft-SAFT Equation of State. *Ind. Eng. Chem. Res.* **2001**, *40*, 2532.

Received for review April 21, 2008
Revised manuscript received August 11, 2008
Accepted August 25, 2008

IE800651Q